Available online at www.sciencedirect.com

ScienceDirect

Journal of Natural Gas Geoscience 1 (2016) 373−382

http://www.keaipublishing.com/jnggs

Original research paper

An insight into the mechanism and evolution of shale reservoir characteristics with over-high maturity☆

Xinjing Li [a,*], Gengsheng Chen [b], Zhiyong Chen [a], Lansheng Wang [b], Yuman Wang [a], Dazhong Dong [a], Zonggang Lü [b], Weining Lü [a], Shufang Wang [a], Jinliang Huang [a], Chenchen Zhang [a]

[a] *Research Institute of Exploration and Development, PetroChina, Beijing 100083, China*
[b] *Southwest Oil and Gas Field Company, PetroChina, Chengdu 610041, China*

Received 28 July 2016; revised 18 September 2016
Available online 10 November 2016

Abstract

Over-high maturity is one of the most vital characteristics of marine organic-rich shale reservoirs from the Lower Paleozoic in the south part of China. The organic matter (OM) in shale gas reservoirs almost went through the entire thermal evolution. During this wide span, a great amount of hydrocarbon was available and numerous pores were observed within the OM including kerogen and solid bitumen/pyrobitumen. These nanopores in solid bitumen/pyrobitumen can be identified using SEM. The imaging can be dissected and understood better based on the sequence of diagenesis and hydrocarbon charge with the shape of OM and pores. In terms of the maturity process showed by the various typical cases, the main effects of the relationship between the reservoir porosity and organic carbon abundance are interpreted as follows: the change and mechanism of reservoirs properties due to thermal evolution are explored, such as gas carbon isotope from partial to complete rollover zone, wettability alteration from water-wet to oil-wet and then water-wet pore surface again, electrical resistivity reversal from the increasing to decreasing stage, and nonlinearity fluctuation of rock elasticity anisotropy. These indicate a possible evolution pathway for shale gas reservoirs from the Lower Paleozoic in the southern China, as well as the general transformation processes between different shale reservoirs in thermal stages.

Keywords: Over-high maturity; Shale gas reservoirs; Solid bitumen; Property

1. Introduction

In the progressive process of thermal evolution, the physical and chemical properties of organic matter are thought to vary [1]. Today, with the evaluation, exploration, and exploitation of shale reservoirs in the world, new evidence related to thermal maturation have been noticed gradually; evidence include organic matter pores, carbon isotope rollover, electrical resistivity reversal, and Thomsen parameters [2−6]. For the Lower Paleozoic marine shale reservoirs in South China, organic matters are involved in a wide range of thermal evolution steps from the early diagenesis through catagenesis, even into metamorphism. They are prominently characterized by an extremely high degree of thermal maturity in dry-gas window rank. Therefore, organic matter and inorganic minerals, theoretically, are subjected to intense transformation in this situation; as kerogen is turned into well-ordered structural materials through polymerization, condensation, and rearrangement reaction, maceral vitrinite gained a strong anisotropy, and an

☆ This is English translational work of an article originally published in *Natural Gas Geoscience* (in Chinese).The original article can be found at: 10.11764/j.issn.1672−1926.2016.03.0407.

* Corresponding author.
E-mail address: xinjingli@petrochina.com.cn (X. Li).

Peer review under responsibility of Editorial office of *Journal of Natural Gas Geoscience*.

http://dx.doi.org/10.1016/j.jnggs.2016.11.001

amount of natural gas along with solid bitumen is generated when the vitrinite reflectance (*R*o) is more than 2% [7,8]. At the time, the processes of inorganic mineral precipitation, cementation, dissolution, recrystallization, and replacement take place, as well as the ordered alteration and preferred orientation of clay minerals occur. The matrix pore size and structure of shale reservoirs have also changed. Nevertheless, the questions associated with how thermal maturity at different stages influence shale properties and reservoir quality, and further makes them specific targets, are yet to be understood and answered.

On the basis of the entire maturity path observed from the incorporated international outstanding cases through the key reservoir parameters, this paper presents the combined effects produced by thermal maturity on shale porosity, wettability, resistivity, elastic anisotropy, and isotopic reversal of natural gas. In the meantime, the research shows intrinsic signatures for shale reservoirs with over high thermal maturity, that is called thermal maturity effect, in order to determine the dynamic features and processes of the Lower Paleozoic marine shale reservoirs from the southern China.

2. Reservoir pore space and carbon isotope for shale gas

2.1. Porosity and nanopores in shale cores

For core samples, conventional core test, mercury injection capillary pressure (MICP), surface area, GRI method, digital imaging technique, and other new means can be used for the laboratory analysis and interpretation of shale porosity. Nevertheless, data from multiple sources are unworkable since they are not interchangeable. For example, MIP results from the examined amount of Hg injected during the testing of the Barnett shale is 20%−50% less than the measurement of the He porosity, because mercury cannot enter the pores connected with 3.6 nm, as well as those with less pore throat. The GRI method, which is recognized internationally, might deviate due to non-unified processing procedures and quality control standards in laboratories. Generally, the difference is 0.5−1.5p.u. [9]. In this study, GRI method data available from mature shale reservoirs of international major areas and strata is still selected to introduce a linear cross-plot between helium (He) porosity and organic matter abundance (Fig. 1). These porosity data chiefly ranges 2%−10%, and 10%−17% in the minority group, and that the amplification of He porosity is different in distinct sections of the organic matter abundance even though the general relationship is positive. In the less abundant area (TOC < 5%), the amplification is great. For example, the correlation coefficient of the Marcellus shale is 0.82−0.86 [10]. However, the correlation in a greater abundant area (TOC > 5%) is usually relatively poor, or even completely irrelevant, regardless of the level of shale maturity. This indicates that the organic matter pore is only one of the important parts of reservoir pore system and that other factors should also be considered.

First, the mineral compositions of organic-rich shale vary. Some are clastic rocks that are constituted mainly by clay mineral and quartz, such as the Longmaxi shale, Marcellus shale, Barnett shale, and Haynesville shale. Some are carbonate rocks with a small amount of quartz, feldspar, clay minerals such as the Green River shale, Eagle Ford shale, Niobrara shale, and Shahejie shale from the Liaohe Depression. In addition to a lot of pores in organic matter, mineral matrix intergranular pore, and intragranular pore are also well developed. For instance, the Eagle Ford shale is characterized by intergranular dissolved pores and cracks, and the Longmaxi shale presents a number of residual intergranular pores (Fig. 2).

Secondly, the kerogen patches are composed of various microscopic compositions without any unified structure. Since kerogen types are different, the relative proportions of chitin group, lipid group, vitrinite group, inertinite group, and others as well as the ability to form organic matter pore also varies. The micro component of the congenital inert is associated to the dead carbon material caused by the reduction of hydrogen in the thermal evolution process. Although they lack the activity and the hydrocarbon generation potential is in limited condition [12], the contribution of these two to organic matter pores are entirely different. Under the microscope, it is common to see organic matter with poor pore development (Fig. 3a−d). By setting the gray level threshold of the SEM images, the delimitated area is extracted. The surface porosity of organic-rich Longmaxi shale with an over high thermal maturity is 24.7% (Fig. 3e and f). Based on more samples from the Longmaxi shale, the porosity value is commonly 7%−30% [4]. For the Barnett shale from the core area, the distribution density and shape of micro and nano-organic pores are inferior than those of the classic style in the published literature (Fig. 3c) [4]. For one of the Woodford mature shale (*R*o = 1.23%), there are no organic matter pores adjacent to the porous area on the micrometer scale. The former may be pyrobitumen, and the latter may be kerogen patches (Fig. 3d) [5]. Noticeably, the same can be observed in the intergranular and intragranular pores in the mineral matrix; additionally, the distribution of organic pore is also heterogeneous.

Third, in the late stage of oil generation, crude oil starts cracking to generate a lot of organic matter pores. Some cavities are connected with narrow throats to form a larger pore network. Even if shale samples come from a larger burial depth, the organic pore morphology remains intact without any deformation (Fig. 3e). It seems that the porosity development in the mineral matrix is considered to be primarily related to the compaction, dissolution, cementation, recrystallization, etc. The creation of organic matter pores has a closer connection to the evolution of thermal decomposition of organic matter during the burial diagenesis and catagenesis.

If it is presumed that the kerogen converted the liquid or gaseous hydrocarbon, organic matter pores produced are controlled dominantly by the maturity, the secondary pores and their specific surface area does not maintain fixed value, which depends on the rearrangement degree of the kerogen structure and expulsion efficiency of hydrocarbon [1]. Thus the required migration pathways for oil and gas inside or nearby source rock would be inseparable with the key parameter. That is to say, in addition to the presentation of pore size, shape, density, and others, the mineral matrix pores well developed in shale

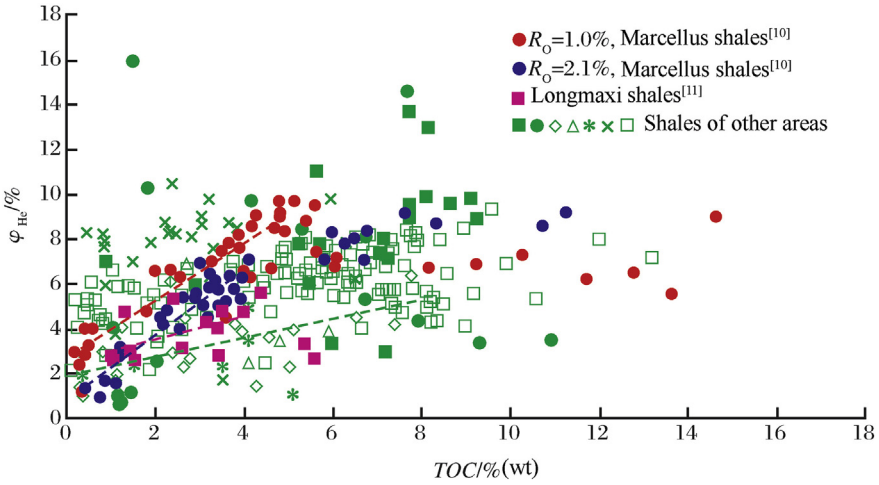

Fig. 1. Correlation between total organic carbon (TOC) abundance and total porosity.

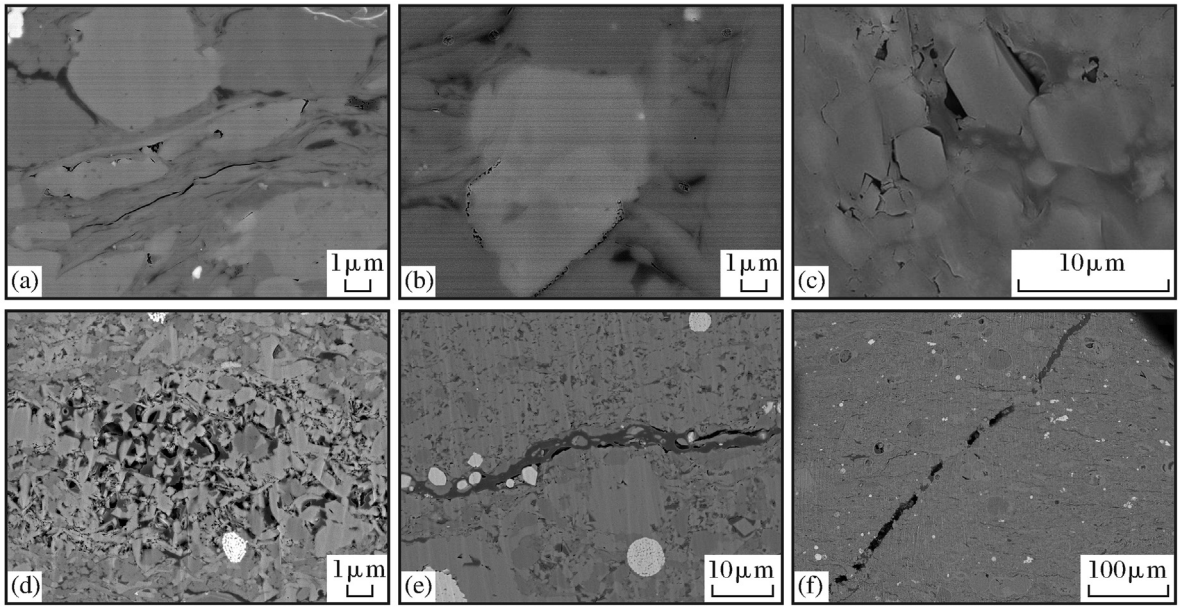

Fig. 2. SEM photomicrograph of intergranular and intragranular pores in the shale matrix; (a) Residual primary intergranular pores in Silurian Longmaxi shale (S_1l) from the Sichuan Basin; (b) Intergranular dissolution pores around carbonate grains in Longmaxi shale from the same area above; (c) Intergranular pores around quartz particles in Tertiary lacustrine shales (ES_4s) from Shahejie Fm. of Bohai Bay Basin (the photo was provided by Ding Wenlong); (d)−(f) Secondary intergranular dissolution pores, interlayer dissolution crack, and organic matter partly filling in dissolution crack in the late stage.

reservoirs also get involved in the heterogeneity phenomenon of organic pore distribution in the view of oil and gas migration.

2.2. Organic nanopore subtypes

The organic matter pore has a close relationship with the hydrocarbon generation and expulsion of shale reservoirs [5,12,13]. The hydrocarbon generation pressurization makes the oil and gas generated from kerogen degradation to displace around the macropore throat to comprehensively fill into the intergranular residual pore of the shale in the diagenetic stage, form a continuous organic matter network, subsequently these result in a large amount of mature and dense shale pores retained in situ and a close-distance migration of liquid hydrocarbon, it also produces solid bitumen/asphalt coke at a higher thermal evolution (Ro >1.1%−1.3%) [14−16], they preserve the nano-pores and micro-cracks, and lastly they become the site of oil and gas accumulation, migration, and production channels [17]. Bernard et al. [18,19] utilized synchrotron scanning transmission X-ray microscope (STXM) to study immature, mature, and over-mature Jurassic Posidonia shale in Germany. The experiments showed that there are indeed molecular solid bitumen and pyrobitumen in the organic matter of mature and over-mature samples. A large amount of sponge-like grain porous is spread in the pyrobitumen. They may be evolutionary intermediates, i.e. residual liquid hydrocarbons. This is the result of gas desolvation in the thermal cracking process. Although it's collectively referred to

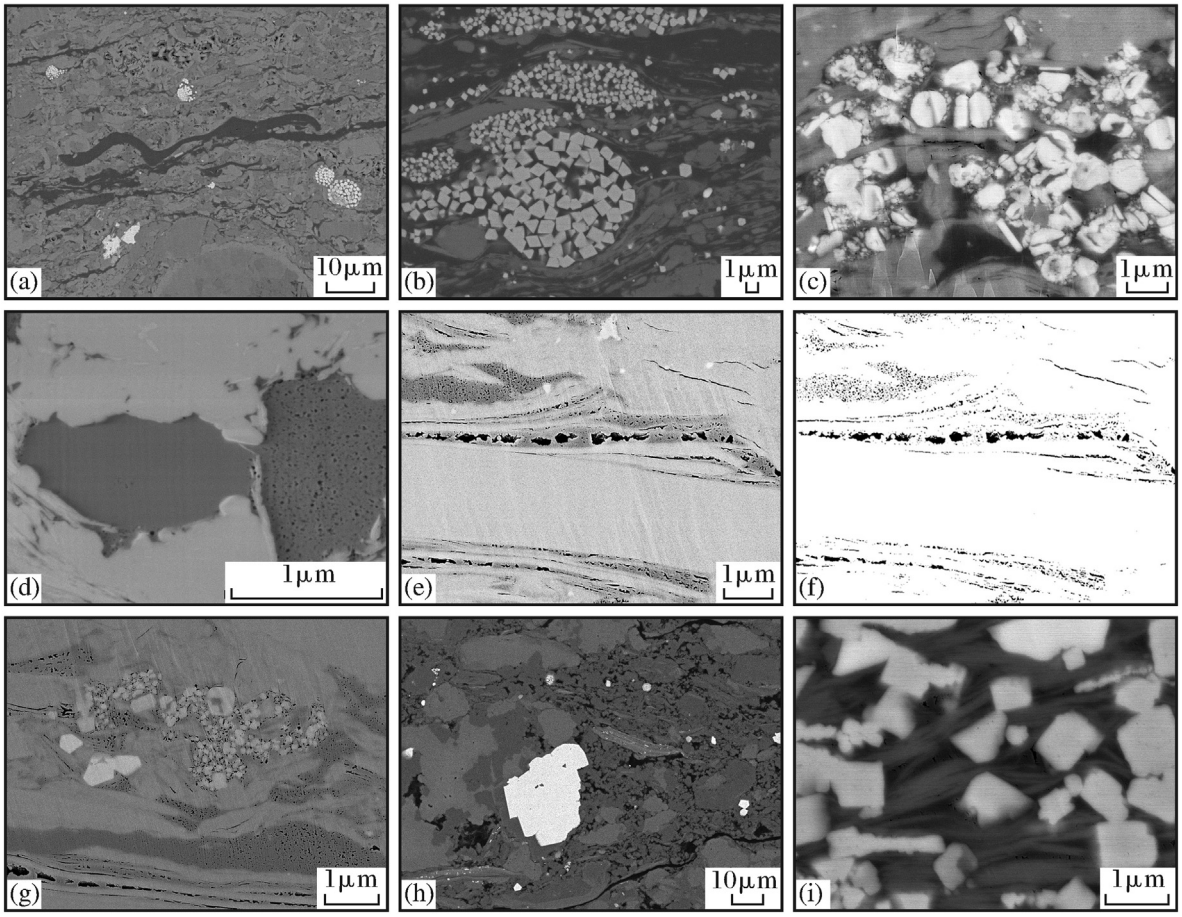

Fig. 3. SEM photomicrograph of organic matter and pores distribution in maturity stages. (a) Immature-lower mature organic matter distributed along the layer in Cretaceous Eagle Ford shale; (b) Multi-layered organic matter (Ro = 0.8%−1.0%) and clay being alignment distribution during early diagenetic compaction in lacustrine Chang 7 shale from Triassic Yanchang Fm. in Ordos Basin; (c) Organic matter pores developed poorly (Ro = 1.9%−2.2%) in Barnett shale from the core area; (d) Organic matter pores showing heterogeneity characteristics in Woodford shale (Ro = 1.4%) [5]. Intergranular pore spaces surrounded by quartz and calcite and filled with solid bitumen/pyrobitumen without organic matter pores in the left side of that; (e), (f) Organic matter pores with 24.7% porosity in thin section of high mature Longmaxi shale (Ro > 2.0%) from the Sichuan Basin; (g) Organic matter pores and intergranular pores in inorganic minerals from the same area above; (h) Intergranular mineral pores and cracks as oil and gas primary migration pathway, filled with bitumen in Longmaxi shale from the same area above; (i) Authigenic pyrite monocrystal and organic matter pores produced during gas generation stage inside kerogen, solid bitumen/pyrobitumen in dual structure of organic matter and clay, from over-mature Qiongzhusi shales (Ro > 2.0%) of the Sichuan Basin.

herein as solid bitumen or pyrobitumen, there are many geological origin types of solid bitumen and a lot of controversy on the classification from the low maturity stage (Ro = 0.35%−0.60%). The paper shows temporary concern on the post-oil solid bitumen relating to liquid hydrocarbon, which is different from kerogen and bitumen absorbed on its surface [17]. As noted earlier, post-oil solid bitumen is derived from liquid hydrocarbon generated in the oil generation phase and is the result of endogenous filling, migration, and more in-depth thermal alteration. Its appearance is usually amorphous, and its forms depend on the occupied pore space [14,17,20,21]. As for the over high mature stage, whether the total rock pore volume, pore size distribution, and the relative ratio of micropores, mesopores, and macropores are changed or reversed, it's still required to perform a lot of research works in the near future. In the past, the main reason why the contribution of solid bitumen has been ignored is that this type of secondary pore is not easy to be identified in a self-sourced reservoir system. Even with the STXM nowadays, it is still not realistic to be widely and quickly practiced in the industry. Integrated with topographical features of solid bitumen in the SEM backscattered image, the sequence of diagenetic evolution, and hydrocarbon charging history, this study attempts to identify them via illustrating some examples.

In Figs. 2 and 3, the presence of long and narrow intergranular aperture with high permeability are observed in the Chang 7 shale from the Ordos Basin, meanwhile, the Eagle Ford shale, Barnett shale, Woodford shale, and Longmaxi shale from the Sichuan Basin. These narrow cracks filled with bitumen, which is accompanied by the formation of substantial nanometer-sized pores in the partial area, are hardly continuous propagation through the field of vision (Fig. 2a, e, 3a, b, g, h). Pyrolysis experiments in Fig. 4a confirmed that oil droplets generated from Woodford shale after heating for four days at 350 °C are exuded from the matrixes and it migrates along the micro-pore direction of high permeability [22]. In Fig. 4b, Biogenic siliceous particles of the Barnet shale occurred as a result of the extensive recrystallization [9] and Passey pointed out that the

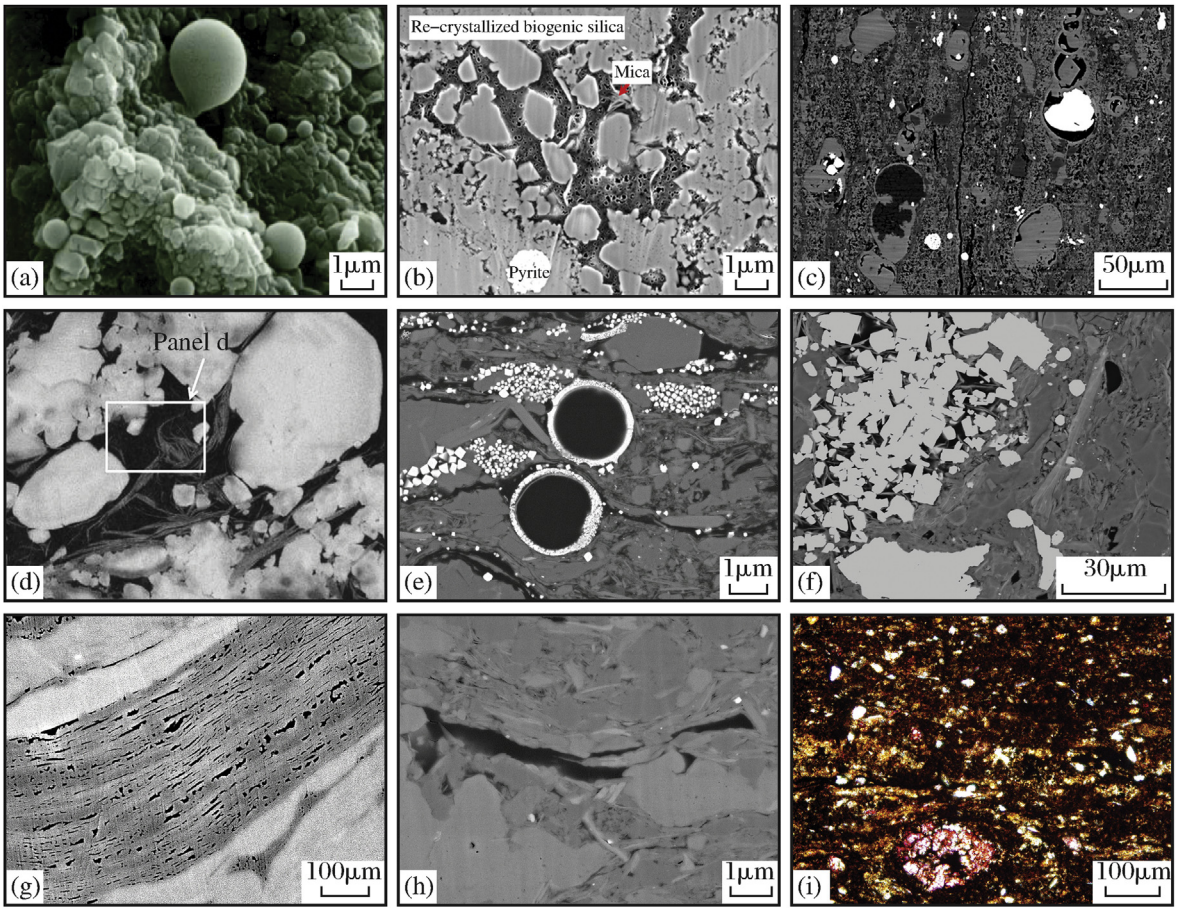

Fig. 4. SEM and thin section photomicrograph of the pores inside solid bitumen and pyrobitumen. (a) Oil droplets around micro-crack produced by the pyrolysis of the Woodford shale [22]; (b) Recrystallization of siliceous minerals and solid bitumen/pyrobitumen pores in the darkest area in Barnett shale [9]; (c) Biogenic body cavity pores of Foraminiferal and matrix pores filled with bitumen in the Eagle Ford shale; (d) Intergranular pores with solid bitumen or pyrobitumen pores in Longmaxi black shale from Pengshui region [11]; (e) Intergranular pore and high permeable channel filled with liquid hydrocarbon during oil generation stage in Chang 7 shale from the Ordos Basin; (f) Intergranular pores filled with pyrite single-crystal aggregates and authigenic clay minerals and residual pores filled with bitumen in Longmaxi shale from the Sichuan Basin; (g) Organic matter pores being alignment distributed along the layer of Longmaxi shale from the same area above; (h) Oil and gas migration phenomenon in intergranular pores and the sponge-like nano-pore network in solid bitumen/pyrobitumen in Longmaxi shale from the same area above; (i) Biogenic siliceous minerals replaced partly by calcite, dissolution pores and surrounding narrow cracks filled with solid bitumen in Longmaxi shale.

dark areas in the picture are the organic matter pores. As a matter of fact, they should be solid bitumen/pyrobitumen pores generated under the higher mature condition by thermal cracking of migration hydrocarbon which is charged after recrystallization of minerals. Fig. 4c presents remarkable diagenetic feature that proves those are carbonate cementation followed by the formation of authigenic pyrite and euhedral as well as semi-euhedral crystalline carbonate within the body cavities of the Foraminifera in the Eagle Ford shale. Subsequently, residual pores are filled with bitumen. In the meantime, intergranular and intragranular dissolution pores, as well as micro-fractures filled with bitumen are also well developed in the mineral matrix. For the Silurian Longmaxi black shale in the Pengshui area, the buried depth is 2149.72 m, the maturity (*R*o) is 2.84%, the organic matter abundance is 3.98%, and the porosity is 4.74% [11]. There are euhedral carbonate crystals in intergranular pores and the dark portion is actually solid bitumen/pyrobitumen pores (Fig. 4d). In Chang 7 black shale of the Triassic Yanchang Formation from Ordos Basin, pyritized coated algae microcyst gradually formed during the pene-contemporaneous and shallow burial stages, along with pyrite crystal aggregates in diagenetic stage and liquid hydrocarbons filled into matrix pores and surrounding channel with high permeability in oil generation stage (Fig. 4e). For the Longmaxi black shales in the Sichuan Basin, SEM and thin section photomicrograph demonstrate residual intergranular pores with irregular shapes among authigenic pyrite crystals and authigenic clay minerals (Fig. 4f), typical micrometer-sized clay-organic matter in which kerogen and in-situ solid bitumen/pyrobitumen pores are arranged along bedding planes (Fig. 4g), as well as sponge-like pores with random distribution in solid bitumen located in long and narrow mineral matrix pore system (Fig. 4h). The picture taken by the optical microscope shows that the residual pore space and long striped apertures surrounding is filled with solid bitumen, following the calcite replacement and then the dissolution of biogenetic silica grains (Fig. 4i).

Therefore, on the basis of microscopic petrology, especially authigenic minerals, diagenesis sequence, pore genesis, and

structural characterization, combined with thermal maturation history and organic matter morphology features, the part of solid bitumen/pyrobitumen being amorphous and dispersed could be identified. The solid bitumen/pyrobitumen is from the degradation products of liquid hydrocarbons generated in oil window. They created a number of high-density and sponge-like solid bitumen/pyrobitumen pore network well connected in the further thermally mature stage due to the thermal decomposition of oil to natural gas. It indicates that mineral matrix pores, microcracks, and organic matter pores containing the pores of kerogen patches and solid bitumen/pyrobitumen might form as an organic whole on account of internally migrating of oil and gas. In other words, the pores network both in mineral matrix and organic matter are not isolated completely from each other. In this system, a sedimentary model of shale reservoir, three stages of diagenesis, catagenesis, epigenesist, and the history of hydrocarbon generation and expulsion jointly control kerogen type, migration pathways, pores features, and then determine the correlation of organic matter abundance and reservoir porosity. Clearly, thermal evolution is the key point. Its effects are also embodied in other physical and chemical properties of gas-bearing shale reservoirs.

2.3. Carbon isotopic reversal of shale gas

The phenomenon of anomaly isotope reversal of methane, ethane, and propane is usually confirmed by the detail investigation for productive shale gas reservoirs. This is the case for Barnett, Fayetteville, Haynesville, Marcellus, Woodford, and even extremely the higher mature Longmaxi shale gas. These cases reveal that the isotope has a geochemical anomaly with respect to maturity trends universality (Fig. 5). The possible genesis mechanism is that hydrocarbon gasses generated by different precursors, which is primary thermal degradation of kerogen and secondary decomposition of residual oil, are mixed and accumulated in closed systems [23]. When natural gas is degraded thermally from kerogen in the early maturity stage, ethane and propane isotopes are increased synchronously. When the vitrinite reflectance is above 1.5%V*R*o, most of the gas is derived from cracking of the oil generated with a little amount from kerogen cracking. Isotopically lighter is richer than those from kerogen cracking on account of isotopic fractionation in the condition, hence, ethane and propane carbon isotopes rollover occurs. This phenomenon was once used to qualitatively predict the permeability and gas production of the Barnett and Haynesville shale reservoirs [24]. Hao (2013) further stated that the relatively lower expulsion efficiency of hydrocarbon and subsequently brings lower loss amount in closed systems during the oil and gas peak generation led to the reversal isotope [23].

When the vitrinite reflectance is greater than 2.0%V*R*o, the late methane generation in relatively closed systems is the result of differentiate kinetic processes: kerogen degradation, oil and wet gas cracking reactions. Methane from oil and wet gas cracking is a major constituent of the hydrocarbon gas. Consequently, the completely isotope rollover appears (Fig. 5 IV). As shown in the figure, compared with isotopically normal of methane, ethane and propane (Zone I), isotopically rollover undergoes three distinguishing zones, namely partially rollover zone II ($\delta^{13}C_2 < \delta^{13}C_1 < \delta^{13}C_3$), partially rollover zone III ($\delta^{13}C_2 < \delta^{13}C_3 < \delta^{13}C_1$) and complete rollover Zone IV ($\delta^{13}C_3 < \delta^{13}C_2 < \delta^{13}C_1$) during the higher over-mature stage. Typical examples of the zones are shown respectively as follows: Barnett in kerogen degradation stage (Zone I), Barnett in oil cracking to gas stage (Zone II), Fayetteville in wet gas cracking stage (Zone III), Marcellus, Horn River, Utica and Longmaxi in later wet gas cracking stage (Zone IV) [23–29]. As can be seen above, the thermal evolution trajectory of stable carbon isotopic compositions of natural gasses, on one side, reflects the complexity of thermal kinetics, isotopic fractionation, oil and gas mixing and accumulation in relatively closed systems [25]; on the other, it reveals that pre-rollover zone in oil cracking to gas stage and post-rollover zone in wet gas cracking stage are two key moments for shale gas accumulation. They carry specific chemical information respectively between the two specific phases. Thus, the gas in the pre-rollover zone is from the products in medium phase of thermal evolution, while the gas in post-rollover zone is from the products in last phase of increasing thermal evolution. Moreover, a certain extent variation on petrophysics signatures of shale reservoirs as below

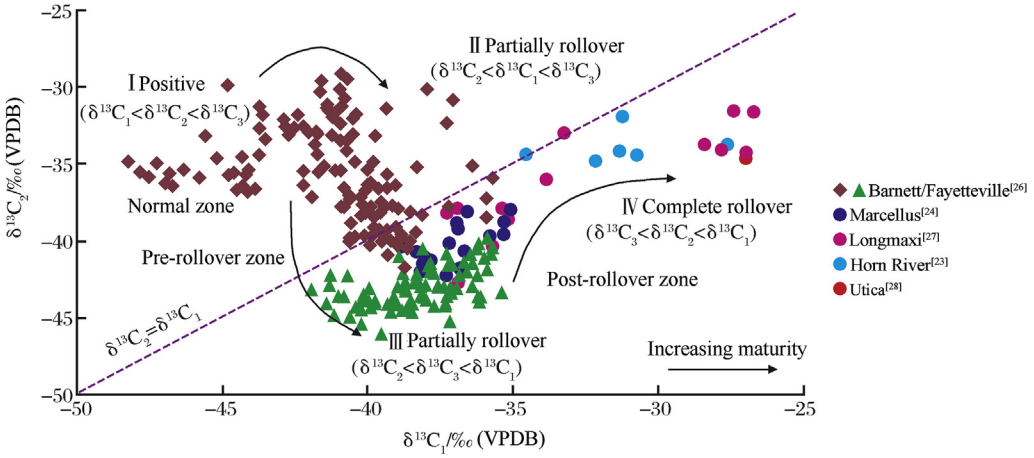

Fig. 5. Compiled carbon isotopic variation of shale gas across the path of thermal maturity (modified from Ref. [23–27,29]).

might also be the result of responding to multiple thermal phases in the view of kerogen transformation in respective opposite direction, which is progressively thermally decomposition and aromatization.

3. Evolution of shale reservoirs characteristics

3.1. Shale reservoir resistivity

Due to additional conductivity of clay mineral and pore water conductivity, immature shales present a low resistivity. With maturity increasing, generated hydrocarbon can displace conducting pore water, pore space and cracks are saturated by oil progressively, and hence shale resistivity increase. Using the correlation between the resistivity and maturity, Schmoker and Hester (1988) [30] defined the resistivity value more than 35 Ω m as a given beginning stage of generating significant amounts of liquid hydrocarbons, delimitated the distribution of mature Bakken shale and Woodford shale. Following in the same way, resistivity of upper and lower Bakken shale located in the northern and western Nesson Anticline are abnormally high (>25,000 Ω m), on account of regional stress and local high heat flow of Brockton-Froid-Fromberg fault zone along NE direction controlled by related basement structures, adjacent to the Trans Hudson Orogen of southeastern of Saskatchewan in Canada [31].

However Passey et al. (2010) [9] observed that the resistivity of some over high mature organic-rich shales (Ro > 3%) was 1−2 orders of magnitude less than that of the lower mature shale (1% < Ro < 3%). Take, for example, Niobrara formation. Shallowly buried Cretaceous Niobrara formation at the edge of Sand Wash Basin is immature thermally with lower pore pressures and resistivity. In oil-generation window along western down dip Sand Wash Basin, the resistivity of target zone gradually increases, which is more than 70 Ω m, and overpressure condition is produced. But in dry gas window of source rock located in further westward basin with high gas-oil ratio, the resistivity is reversely dropped to 40−50 Ω m [32]. Oil companies typically regarded the area which is more than 30 Ω m as potential regional object of Niobrara shale oil and gas exploration. Another example is Woodford shale in Arkoma Basin and Anadarko Basin. With increasing maturity, the resistivity ranges up to over 500 Ω m, with highest 1000 Ω m from lower than 20 Ω m and then down to 10−15 Ω m in the dry gas zone. Bakken shale in Williston Basin also has the similar trend as displayed universally by the cases above (Table 1).

In the evolution level from wet gas window into dry gas window, why does the resistivity reverse? At present, there are mainly several viewpoints as follows: (1) Graphite precursor produced in highly thermal mature stage. This view is thrown into doubt, for a similar phenomenon occurs also at about 1.4%VRo [9,33]; (2) Decreased resistivity of formation water (Rw) caused by vaporization of irreducible water. The salinity of residual water is increased as efficient removals of water through vaporization, and then Rw value of shale formation is reduced. Resistivity inversion happens [34]; (3) Wettability alteration. Schmoker and Hester (1988) believed that the effect of conventional factors such as pyrite and clay mineral, porosity, pore tortuosity and the salinity of pore water would be secondary, compared with the thermal maturity. In wet gas window, liquid hydrocarbon is decomposed gradually and oil wettability of solid bitumen/pyrobitumen is transformed to water wettability due to structure change. Hence, shale resistivity is reversed in over-high mature level [30]; (4) Microcrack presence. Al Dhhailan et al. (2014) pointed out that the crack porosity might be 5% per 50Ma, generated during a large amount of oil generation and expulsion stage, and 1% excess porosity during the gas generation stage. Furthermore, with the effect of variable Archie saturation exponent n, a decrease in the resistivity amplitude may be up to 80% [32].

According to the process analysis of thermal evolution and the primary migration of continuous phase (crude oil) fluids, the paper supports the mechanism on wettability change. During the immature-low mature stage, the shale resistivity is controlled by the continuous phase of pore water which is in a low resistance situation. During the oil generation stage, non-polar liquid hydrocarbon and polar organic fractions (asphaltenes and resins) is produced because of thermal cracking of kerogen. While the generated non-polar hydrocarbon as continuous phase displaces water to occupy the center of pore space, polar organic compounds compete with water phase to cover the surface of inorganic minerals, alter the rock wettability gradually till that the continuous aqueous phase is interrupted and the resistivity is increased significantly. When the thermal maturity keeps rising, the thermal cracking of wet gas dominates and produces high pressure and micro cracks resulted from volume expansion of fluids within the source rock. The connectivity of pore system and the capacity of expelling hydrocarbon are enhanced. In the meantime, asphaltenes and resins are detached and dispersed. The water-wet system isolated before is reconnected and the surface of minerals is occupied again by irreducible water which triggers oil-wet state on black shale reversal and formation conductivity recovered.

Table 1
Resistivity of shale reservoirs in the range of thermal maturity.

Target interval	Niobrara [32]		Bakken [31]	Woodford [30]	Longmaxi
Basin	Sand Wash	Piceance	Williston	Anadarko/Arkoma	Sichuan
Immature stage Rt/(Ω m)	<10	/	7−9	20−35	/
Oil generation stage Rt/(Ω m)	<20 (early stage), 40−60 (late stage)	10−16	>35	>35	/
Wet gas stage Rt/(Ω m)	90−120 (>70)	>30	25000 (max)	100−500, > 1000 (max)	/
Dry gas stage Rt/(Ω m)	40−50	18−22	/	10−15 (shallow well)	25−140, 200 (max)

Even very low water saturation now is able to decrease the resistivity of shale reservoirs enough. Thus, compared with the major shale reservoirs in North American, Longmaxi shales in southern China with over high mature enter almost at the end of completely thermal evolution sequence, the part of mineral surface has been reversed into water-wet state. Shale reservoirs generally are characterized by lower formation resistivity (Table 1). It also shows the importance of primary hydrocarbon migration, expulsion and accumulation inside and/or nearby source rocks during the generation phase of the amount of oil and gas. Tight oil and gas reservoirs in Middle Bakken section with high yield and low resistance are typical accumulation of near-source rock. Shale strata with high resistivity in Bohai Bay Basin, Songliao Basin, Ordos Basin and others that are in the oil generation stage may similarly be also the exploration targets for tight reservoirs with relatively lower risk.

3.2. Shale reservoir anisotropy

Compared with sandstone and carbonate rocks, the intrinsic anisotropy of organic-rich shale is relatively stronger. It is necessary to consider the features for calculating elastic parameters, such as Young modulus and Poisson's ratio, and quantifying fracturability or brittleness parameters. But representative experimental data overlapped organic matter richness with maturity factor is relatively limited, and the variation of Thomson parameters is not very clear, especially in the high thermal maturation. The stress sensitivity experiment of organic-rich shale by Vanorio et al. (2008) is pretty worth of preliminary reference. It shows two distinct characteristics [35] (Fig. 6a): 1. Shale anisotropy response to the stress in different mature ranges appears to be different. In the lower maturity stage ($Ro < 0.65\%$), Thomson parameter ε denoting P-wave anisotropy is increased monotonously with the rising maturity, but stress sensitivity is weak. Thermal maturity turns into primary controlling factor. After the peak hydrocarbon generation, when stress magnitude is increased from 5 MPa into 50 MPa, ε is decreased trend in the whole core samples, and the stress also becomes one of controlling factors. 2. The reversal of Thomson parameter occurs at oil generation ($Ro = 0.65\%$) and peak gas generation ($Ro = 1.3\%$) and anisotropy strength varies nonlinearly. In this paper, combined these results with experimental data under 50 MPa circumstances from Deng et al. [36] to cite anisotropy characteristics of Wufeng−Longmaxi black shales at over high maturity range in Upper Yangtze Region of South China, the change of rock physics properties in integrated maturity sequence could be observed, considering regional thermal maturity levels ($Ro > 2.0\%$) where the samples are located. The graph indicates that ε parameter still gives a general proof of the fluctuation with slightly downward trends, in addition to the high value of individual samples (their clay content reach up to about 40%). The reason why the amplitude of parameter fluctuation around the maturity in 2.0% is much more, might be related to the quite difference of clay content for Longmaxi shales in Yangtze Region. It might indicate that structure development and characteristics of the organic matter have nonlinear change in the whole thermal evolution. Moreover, the effect of other controlling factors should be under consideration on the anisotropy of shale reservoir, in addition to the maturity. More detailed explanation is given below.

Fig. 6b and c bring out the strong correlation between the over high mature Longmaxi shale clay mineral content and the anisotropy parameters of P and S wave (ε and γ). In the array of clay mineral content lower than 30%, ε slowly goes up with the increasing clay content. On the other hand, clay mineral whose

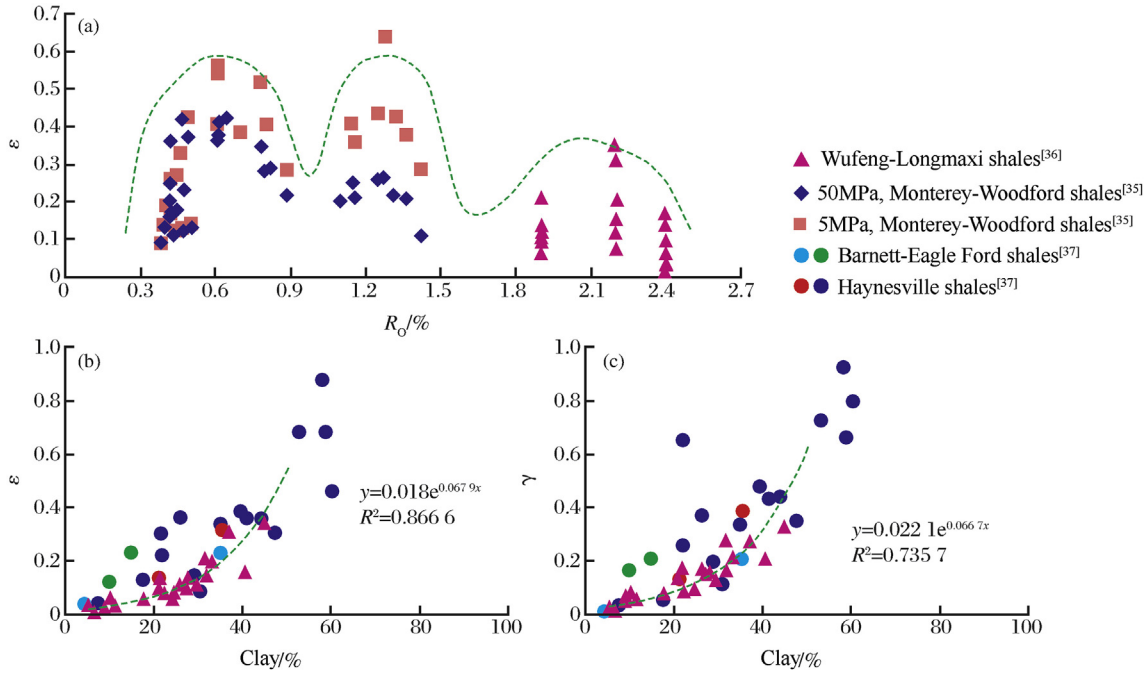

Fig. 6. Thomson parameter ε variation across thermal maturity (a), Plots of Thomson parameters (ε, γ) versus clay content (b), (c).

content is more than 30% causes the anisotropy to move up sharply. This phenomena are consistent with the general trend of the Haynesville shale, Barnett shale, and Eagle Ford shale [36,37]. Qin et al. (2014) set the mature Bakken shale as an example to calculate the influence of organic matter abundance and maturity on the elastic rock parameters of physical rock such as the acoustic velocity, P-to-S velocity ratio, and anisotropy, under the hypothesis and mathematical models [38]. The results show that the rock anisotropy appreciates with the increasing maturity and organic matter content; Vp/Vs ratio of shale reservoirs decreases with the heightened maturity, when the organic matter abundance is higher ($V_{TOC} > 25\%$). When the abundance of organic matter is relatively low ($V_{TOC} < 25\%$), the TOC content has a relatively stronger influence on the elastic parameter ε of shales. In this situation, sedimentary environment of organic-rich shales and terrigenous supply could have a strong constraint on the original background value of ε. Theoretically, flocculated aggregates of organic matters and clay particles deposit in relatively weak hydrodynamic conditions. Clay particles and low-density organic matter are dehydrated gradually, which eventually aligns parallel to the bedding planes during diagenetic compaction. And then the number of clay-organic matter lamina structures lead to further strengthening of the shale anisotropy. During a large amount of hydrocarbon generation and expulsion stage, increasing fluid pressure due to kerogen-to-oil and oil-to-gas conversion in organic-rich shales induces microcracks in source rocks. Meanwhile, kerogen progressively begins a higher degree of polycondensation, the pores of kerogen and solid bitumen/pyrobitumen are developed, and organic materials are dispersed at the appropriate time. It turns out that P and S wave velocity, P-to-S velocity ratio, and anisotropy of original-rich shale reservoirs in the range of thermal maturity come into being the process of non-linear transformation.

In brief, anisotropy property of organic-rich shales is controlled by many factors such as hydrodynamic conditions, sediment provenance, burial diagenesis, variations in organic matter composition and structure exposed to temperature and pressure during the maturation process, and stress fractures including micro cracks. They exert influence on different scales. The way to describe the anisotropy of organic-rich shales depends on the research purpose and the questions required to solve. In addition to the maturity, it is necessary to integrate geological factors to know well the features of organic-rich shale reservoirs in the southern China.

4. Conclusions

(1) The pores of organic matters in shale reservoirs include kerogen pores and solid bitumen/pyrobitumen pores. It is helpful for identifying the pore types and getting additional information on the origin and timing of pores and microcracks to eventually take advantage of petrology and diagenesis study. Mineral matrix pores, micro cracks, and organic pores are not completely isolated from each other, but they are moreover integrated. Maceral compositions and maturities of organic matter, as well as the pathway of primary fluid migration, constrain together the extremely heterogeneous distribution and evolution characteristics of organic matter pore networks on a scale of nanometers; this also influence the correlation between organic matter abundance and porosity of shale reservoirs.

(2) The Lower Paleozoic marine organic-rich shale reservoirs in the southern China, compared to those in North America, are characterized by over-high thermal maturity. The cracking of crude oil and wet gas into thermally stable methane hold a dominant position in the evolution pathway. When the evolution scheme was applied to the Longmaxi shales, a large amount of solid bitumen pores was formed, shale gas carbon isotope went into a complete rollover zone, wettability alteration of pore surfaces is from water-wet into oil-wet and again water-wet, reservoir resistivity goes up and down, and rock anisotropy parameters are nonlinear fluctuation. All of the phenomena demonstrate the possible evolving characteristics of the Lower Paleozoic marine organic-rich shale reservoirs in the South China. The occurrences indicate the internal links and changes of shale reservoir features in different mature stages. It is oversimplified to consider that high maturity mainly limits the breakthrough of shale gas exploration and development in the southern China. A complex geologic background is the key to unlocking the potential valuable resource, which should be analyzed and interpreted from the understanding of petroleum system as well as past and present stress field. The practice on the development of Longmaxi black shale in the Sichuan Basin is the typical case.

Foundation item

Supported by National Basic Research Program of China (973) (2013CB228001); National Science and Technology Specific Project (2011ZX05018-001).

Conflict of interest

The authors declare no conflict of interest.

Acknowledgments

The authors gratefully thank the University of Texas at Austin, for providing Eagle Ford and Barnett samples and also Jack Breig for the helpful insight on organic-rich shale wettability.

References

[1] B.P. Tissot, D.H. Welte, Petroleum Formation and Occurrence, Springer-Verlag, New York, 1984, pp. 1−463.

[2] Chunhui Cao, Mingjie Zhang, Mingjie Tang, Zonggang Lv, Yang Wang, Li Du, Zhongping Li, Geochemical characteristics and implications of shale gas Longmaxi Formation, Sichuan Basin, China, Nat. Gas. Geosci. 26 (8) (2015) 1604−1612.

[3] Zhenya Qu, Jianan Sun, Jianting Shi, Zhaowen Zhan, Yanrong Zou, Ping'an Peng, Characteristics of stable carbon iosotopic composition of shale gas, Nat. Gas. Geosci. 26 (7) (2015) 1376−1384.

[4] Xingjing Li, Characteristics of Shale Gas Reservoirs for High Maturity in Sichuan Basin, Resarch Institute of Exploration and Development, PetroChina, Beijing, 2010, pp. 1−79.
[5] M.E. Curtis, B.J. Cardott, C.H. Sondergeld, C.S. Rai, Development of organic porosity in the Woodford shale with increasing thermal maturity, Int. J. Coal Geol. 103 (2012) 26−31.
[6] N. Kethireddy, H. Chen, Z. Heidari, Quantifying the effect of kerogen on resistivity measurements in organic-rich rocks, Petrophysics 55 (3) (2014) 136−146.
[7] B. Durand, G. Nicaise, Procedures for kerogen isolation, in: B. Durand (Ed.), Kerogen—Insoluble Organic Matter from Sedimentary Rocks, Editions Technip, Paris, 1980, pp. 35−53.
[8] Jiamo Fu, Benshan Wang, Jiyang Shi, Rongfen Jia, Guoying Sheng, Evolution of organic matter and origin of sedimentary ore deposites, Acta Sedimentol. Sin. 1 (3) (1983) 41−58.
[9] Q.R. Passey, K. Bohacs, W.L. Esch, R. Klimentidis, S. Sinha, From oil-prone source rock to gas-producing shale reservoir-geologic and petrophysical characterization of unconventional shale gas reservoirs, in: International Oil and Gas Conference and Exhibition in China, Society of Petroleum Engineers, 2010.
[10] K.L. Milliken, M. Rudnicki, D.N. Awwiller, T. Zhang, Organic matter−hosted pore system, Marcellus Formation (Devonian), Pennsylvania, AAPG Bull. 97 (2) (2013) 177−200.
[11] Hui Tian, Lei Pan, Xianming Xiao, Ronald W.T. Wilkins, Zhaoping Meng, Baojia Huang, A preliminary study on the pore characterization of Lower Silurian black shales in the Chuandong Thrust Fold Belt, southwestern China using low pressure N_2 adsorption and FE-SEM methods, Mar. Pet. Geol. 48 (2013) 8−19.
[12] D.M. Jarvie, R.J. Hill, T.E. Ruble, R.M. Pollastro, Unconventional shale gas systems: the Mississippian Barnett shale of north-central Texas as one model for thermogenic shale gas assessment, AAPG Bull. 90 (4) (2007) 475−499.
[13] R.G. Loucks, R.M. Reed, S.C. Ruppel, D.M. Jarvie, Morphology, genesis, and distribution of nanometer-scale pores in siliceous mudstones of the Mississippian Barnett Shale, J. Sediment. Res. 79 (12) (2009) 848−861.
[14] N. Fishman, J. Guthrie, M. Honarpour, Development of organic and inorganic porosity in the Cretaceous Eagle Ford Formation, South Texas, in: 2013 AAPG Annual Convention and Exhibition, American Association of Petroleum Geologists, 2013.
[15] P.C. Hackley, Geological and geochemical characterization of the Lower Cretaceous Pearsall Formation, Maverick Basin, south Texas: a future shale gas resource? AAPG Bull. 96 (8) (2012) 1449−1482.
[16] M. Mastalerz, A. Schimmelmann, A. Drobniak, Y. Chen, Porosity of Devonian and Mississippian New Albany Shale across a maturation gradient: insights from organic petrology, gas adsorption, and mercury intrusion, AAPG Bull. 97 (10) (2013) 1621−1643.
[17] B.J. Cardott, C.R. Landis, M.E. Curtis, Post-oil solid bitumen network in the Woodford Shale, USA—a potential primary migration pathway, Int. J. Coal Geol. 139 (2015) 106−113.
[18] S. Bernard, B. Horsfield, H.M. Schulz, R. Wirth, A. Schreiber, N. Sherwood, Geochemical evolution of organic-rich shales with increasing maturity: a STXM and TEM study of the Posidonia Shale (Lower Toarcian, northern Germany), Mar. Pet. Geol. 31 (1) (2012) 70−89.
[19] S. Bernard, R. Wirth, A. Schreiber, H.M. Schulz, B. Horsfield, Formation of nanoporous pyrobitumen residues during maturation of the Barnett Shale (Fort Worth Basin), Int. J. Coal Geol. 103 (2012) 3−11.
[20] H. Jacob, Classification, structure, genesis and practical importance of natural solid oil bitumen (“migrabitumen”), Int. J. Coal Geol. 11 (1) (1989) 65−79.
[21] J.A. Curiale, Origin of solid bitumens, with emphasis on biological marker results, Org. Geochem. 10 (1−3) (1986) 559−580.
[22] R.M. Slatt, P.R. Philp, Y. Abousleiman, P. Singh, R. Perez, R. Portas, K.J. Marfurt, S. Madrid-Arroyo, N. O'Brien, E. Eslinger, E.T. Baruch, Pore-to-regional-scale integrated characterization workflow for unconventional gas shales, in: J.A. Breyer (Ed.), Shale Reservoirs—Giant Resources for the 21st Century, AAPG Memoir 97, 2012, pp. 127−150.
[23] B. Tilley, K. Muehlenbachs, Isotope reversals and universal stages and trends of gas maturation in sealed, self-contained petroleum systems, Chem. Geol. 339 (2013) 194−204.
[24] J.E. Zumberge, K.A. Ferworn, J.B. Curtis, Gas character anomalies found in highly productive shale gas wells, Geochim Cosmochim Acta Suppl. 73 (2009) 1539−1556.
[25] F. Hao, H. Zou, Cause of shale gas geochemical anomalies and mechanisms for gas enrichment and depletion in high-maturity shales, Mar. Pet. Geol. 44 (2013) 1−12.
[26] J. Zumberge, K. Ferworn, S. Brown, Isotopic reversal (‘rollover’) in shale gases produced from the Mississippian Barnett and Fayetteville formations, Mar. Pet. Geol. 31 (1) (2012) 43−52.
[27] Jinxing Dai, Caineng Zou, Shimeng Liao, Dazhong Dong, Yunyan Ni, Jinliang Huang, Wei Wu, Deyu Gong, Shipeng Huang, Guoyi Hu, Geochemistry of the extremely high thermal maturity Longmaxi shale gas, southern Sichuan Basin, Org. Geochem. 74 (2014) 3−12.
[28] R.C. Burruss, C.D. Laughrey, Carbon and hydrogen isotopic reversals in deep basin gas: evidence for limits to the stability of hydrocarbons, Org. Geochem. 41 (12) (2010) 1285−1296.
[29] X. Xia, J. Chen, R. Braun, Y. Tang, Isotopic reversals with respect to maturity trends due to mixing of primary and secondary products in source rocks, Chem. Geol. 339 (2013) 205−212.
[30] J.W. Schmoker, T.C. Hester, Formation resistivity as an indicator of the onset of oil generation in the Woodford shale, Anadarko Basin, Oklahoma, in: K.S. Johnson (Ed.), Anadarko Basin Symposium, OGS Circular, vol. 90, 1988, pp. 262−266.
[31] L.K. Kreis, A. Costa, Hydrocarbon potential of the Bakken and Torquay Formations, southeastern Saskatchewan, in: Summary of Investigations, Saskatchewan Geological Survey, vol. 1, Sask. Industry Resources, Misc. Rep, 2005, p. A-10.
[32] M.A. Al Duhailan, S. Cumella, Niobrara Maturity Goes up, Resistivity Goes Down; What's Going on? SPE/AAPG/SEG Unconventional Resources Technology Conference, Society of Petroleum Engineers, 2014.
[33] S. Cumella, J. Scheevel, Mesaverde tight gas sandstone sourcing from underlying Mancos-Niobrara shales, Search Discov. (2012) 10450.
[34] K.E. Newsham, J.A. Rushing, Laboratory and field observations of an apparent sub capillary-equilibrium water saturation distribution in a tight gas sand reservoir, in: SPE Gas Technology Symposium, SPE 75710, 2002, pp. 5−8.
[35] T. Vanorio, T. Mukerji, G. Mavko, Emerging methodologies to characterize the rock physics properties of organic-rich shales, Lead. Edge 27 (6) (2008) 780−787.
[36] J. Deng, G. Tang, P. Yan, Microtexture, seismic rock physical properties and modeling of Longmaxi Formation shale, Chin. J. Geophysics Chines Ed. 58 (6) (2015) 2123−2136.
[37] H. Sone, Mechanical Properties of Shale Gas Reservoir Rock and its Relation to the In-situ Stress Variation Observed in Shale Gas Reservoir, Stanford University, California, 2012, pp. 1−247.
[38] X. Qin, D. Han, L. Zhao, Rock physics modeling of organic-rich shales with different maturity levels, in: 2014 SEG Annual Meeting, Society of Exploration Geophysicists, 2014.